LECTURE 13: THE MEASUREMENT OF BAO

GONG-BO ZHAO

Abstract. This lecture keeps the compact 2025 material on the survey window function and BAO fitting, and extends it in the more explanatory 2026 lecture-note style. The new material explains how the survey window can be represented as a binned linear operator, how DESI performs the window operation as a matrix multiplication, why multipole leakage requires theory input beyond the measured multipoles, and how the DESI DR1 full-shape analysis regularizes highly non-diagonal windows produced by the small-angle cut used to mitigate fiber-assignment incompleteness.

Learning goals

After this lecture, students should be able to:

- explain why a survey mask turns the theoretical power spectrum into a convolved observable;
- write the survey-window operation as a binned matrix multiplication acting on power-spectrum multipoles;
- understand why the window mixes both scales and multipoles, and why DESI keeps higher-order theory multipoles in the convolution;
- describe the rotated-window method used in DESI DR1 when the raw window matrix becomes too non-diagonal;
- connect these technical ideas to practical BAO and full-shape analyses in DESI.

1. The survey window function

Due to the geometry of the survey volume, we have to convolve the theoretical power spectrum with the survey window function, which is a pain, but there is no way around it.

$$\delta'(\mathbf{x}) = \delta(\mathbf{x})W(\mathbf{x}), \tag{1}$$

$$\tilde{\delta}'(\mathbf{k}) = \tilde{\delta}(\mathbf{k}) * \tilde{W}(\mathbf{k}), \tag{2}$$

where $*$ denotes a convolution.

$$P'(\mathbf{k}) = \int \frac{d^3q}{(2\pi)^3} P(\mathbf{k}-\mathbf{q})|\tilde{W}(\mathbf{q})|^2 \tag{3}$$

Fortunately, it was found that the 3D convolution can be broken into 1D Hankel transformations, due to the convolution theorem [1].

$$P_\ell(k) = 4\pi(-i)^\ell \int \Delta^2 d\Delta \xi_\ell(\Delta) j_\ell(k\Delta) \tag{4}$$

$$P'_\ell(k) = 4\pi(-i)^\ell \left(\frac{2\ell+1}{2q+1}\right) \times A^q_{\ell,\ell'} \int \Delta^2 d\Delta \xi_{\ell'}(\Delta) Q_q(\Delta) j_\ell(k\Delta) \tag{5}$$

$$RR^{\rm tot}_q(\Delta) = \frac{1}{2}\overline{n}_s^2 2\pi\Delta^3 d(\ln\Delta) Q_q(\Delta) \tag{6}$$

$$\xi'_0(\Delta) = \xi_0 Q_0 + \frac{1}{5}\xi_2 Q_2 + \frac{1}{9}\xi_4 Q_4 + \frac{1}{13}\xi_6 Q_6 + \cdots \tag{7}$$

$$\begin{aligned} \xi'_2(\Delta) = \xi_0 Q_2 &+ \xi_2 \quad \left(Q_0 + \frac{2}{7}Q_2 + \frac{2}{7}Q_4\right) \\ &+ \xi_4 \quad \left(\frac{2}{7}Q_2 + \frac{100}{693}Q_4 + \frac{25}{143}Q_6\right) \\ &+ \xi_6 \quad \left(\frac{25}{143}Q_4 + \frac{14}{143}Q_6 + \frac{28}{221}Q_8\right) \end{aligned} \tag{8}$$

1.1. **From a continuous convolution to a binned linear operator.** The integral equations above are exact, but in an actual likelihood analysis we never compare a continuum theory curve directly to the data. What is measured is a finite set of band powers in a finite set of multipoles. It is therefore natural to package the survey window into a linear operator that maps a theory vector to the expected measured data vector.

Define the measured band power in multipole ℓ and bin i by

$$P^{\rm obs}_{\ell,i} \equiv \frac{1}{\Delta k_i} \int_{k_i^-}^{k_i^+} dk\, P'_\ell(k). \tag{9}$$

Then the convolved prediction may be written schematically as

$$P^{\rm obs}_{\ell,i} = \sum_{\ell'} \int dk'\, W_i^{\ell\ell'}(k')\, P^{\rm th}_{\ell'}(k'). \tag{10}$$

After discretizing the theory on a sufficiently fine grid k_j, this becomes

$$P^{\rm obs}_{\ell,i} \simeq \sum_{\ell',j} \mathcal{W}_{ij}^{\ell\ell'}\, P^{\rm th}_{\ell'}(k_j). \tag{11}$$

If we now stack all measured multipoles into a single data vector,

$$\mathbf{d} \equiv (P_0(k_1), \ldots, P_0(k_{N_d}), P_2(k_1), \ldots, P_2(k_{N_d}))^T, \tag{12}$$

and similarly collect the theory multipoles on the fine grid into

$$\mathbf{t} \equiv \left(P_0(k^{\rm th}_1), \ldots, P_0(k^{\rm th}_{N_t}), P_2(k^{\rm th}_1), \ldots, P_4(k^{\rm th}_{N_t})\right)^T, \tag{13}$$

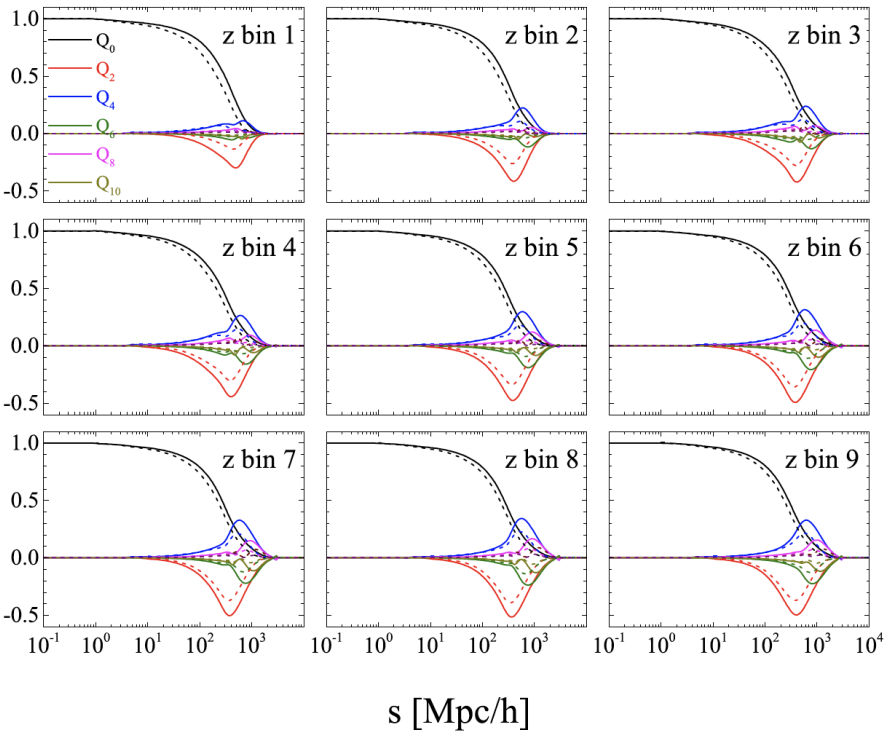

FIGURE 1. The survey window function for BOSS DR12 [6].

then the window operation takes the compact form

$$\mathbf{d}_{\rm th} = \mathbf{W}\,\mathbf{t}. \tag{14}$$

This is the modern DESI-style view of the survey window: all effects of the mask, estimator, binning and line-of-sight convention are precomputed once and stored in a matrix $\mathbf{W}$.

An analogous compression can also be written in configuration space,

$$\xi^{\rm obs}_{\ell,i} \simeq \sum_{\ell',j} \mathcal{W}^{(\xi)\,\ell\ell'}_{ij}\, \xi^{\rm th}_{\ell'}(s_j), \tag{15}$$

but the Fourier-space version is especially convenient because every likelihood evaluation then reduces to a matrix-vector multiplication.

1.2. **Why the window mixes scales and multipoles.** The survey window is not just a multiplicative prefactor. It mixes nearby and sometimes rather distant wavenumbers, and it also mixes multipoles. Schematically,

$$P_0^{\rm obs}(k_i) = \sum_j \left[W^{00}_{ij} P_0(k_j) + W^{02}_{ij} P_2(k_j) + W^{04}_{ij} P_4(k_j) + \cdots \right], \tag{16}$$

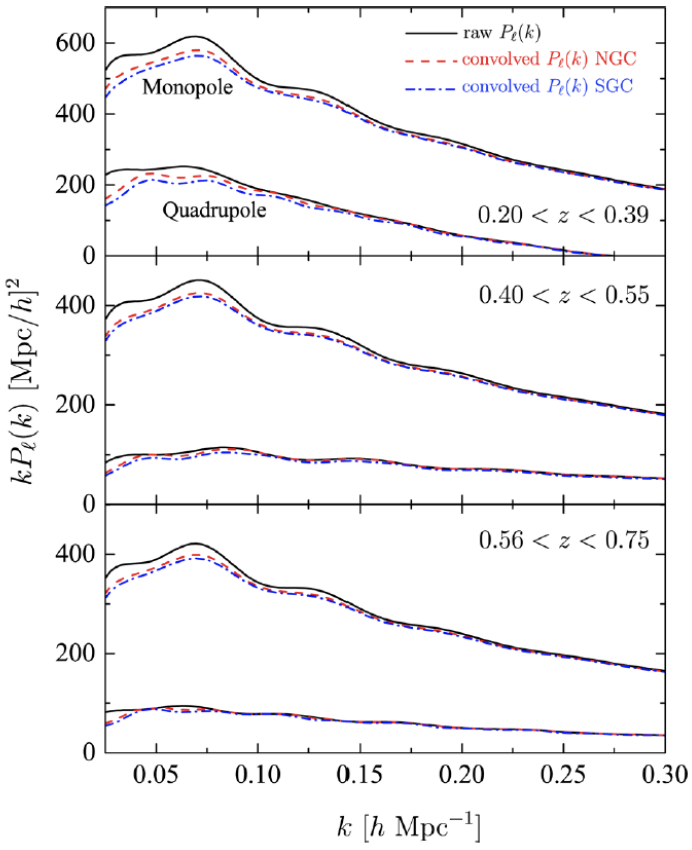

FIGURE 2. The convolved power spectra [6].

$$P_2^{\rm obs}(k_i) = \sum_j \left[W_{ij}^{20} P_0(k_j) + W_{ij}^{22} P_2(k_j) + W_{ij}^{24} P_4(k_j) + \cdots \right] . \tag{17}$$

This is the practical reason that one should not convolve only the same multipoles that are finally displayed in the data vector. Even if the measurement reports only the monopole and quadrupole, higher-order theory multipoles can leak into them through the window. In DESI DR1, the power-spectrum window matrix is estimated from the two-point selection

function measured from the random catalog, and in the power-spectrum case it also includes first-order wide-angle effects [14].

1.3. **DESI example: BAO window convolution by matrix multiplication.** The DESI DR1 galaxy BAO analysis provides a clean example of how this is implemented in practice [9]. The BAO theory model is first constructed in fiducial coordinates, then the model multipoles are convolved with the survey window by direct matrix multiplication,

$$\mathbf{d}_{\rm BAO}^{\rm th} = \mathbf{W}_{\rm BAO}\,\mathbf{t}_{\rm BAO}. \tag{18}$$

In the official implementation the unconvolved theory is evaluated on a computational k-grid that is five times finer than the data binning and spans a somewhat larger k-range than the fitted data vector. Moreover, DESI keeps angular dependence up to at least the hexadecapole in the theory input to the window multiplication, because the mask allows power in these higher multipoles to leak into the observed monopole and quadrupole [9].

This is one of the main advantages of the matrix formalism. Once $\mathbf{W}_{\rm BAO}$ has been measured from the random catalog, each likelihood evaluation only needs a dense matrix-vector product. That is numerically trivial compared to recomputing a full three-dimensional convolution from scratch for every MCMC step or every minimizer call.

1.4. **DESI example: rotated window matrices for full-shape analyses.** For the DESI DR1 full-shape power-spectrum analysis, an additional complication arises from fiber assignment. To mitigate the incompleteness caused by missing close pairs, DESI adopts a small-angle truncated estimator, usually denoted a θ-cut, removing pair contributions below a threshold of about 0.05° [16, 15]. This succeeds in removing the contaminated small-angle pairs, but it also makes the raw power-spectrum window matrix very non-diagonal. As a result, the prediction for observed modes inside the fitting range can receive contributions from theory modes at much higher k than the scales where perturbation theory is trusted.

The starting Gaussian likelihood is

$$\chi^2 = (\mathbf{d} - \mathbf{W}\,\mathbf{t})^T \mathbf{C}^{-1} (\mathbf{d} - \mathbf{W}\,\mathbf{t}). \tag{19}$$

If we apply any invertible linear transformation $\mathbf{M}$ to the data vector, then the likelihood is unchanged provided we transform everything consistently:

$$\chi^2 = (\mathbf{d}' - \mathbf{W}'\mathbf{t})^T \mathbf{C}'^{-1} (\mathbf{d}' - \mathbf{W}'\mathbf{t}), \tag{20}$$

with

$$\mathbf{d}' = \mathbf{M}\mathbf{d}, \tag{21}$$

$$\mathbf{C}' = \mathbf{M}\mathbf{C}\mathbf{M}^T, \tag{22}$$

$$\mathbf{W}' = \mathbf{M}\mathbf{W}. \tag{23}$$

DESI extends this idea slightly further by allowing a rank-1 completion of the window that can be absorbed by an extra nuisance amplitude. Schematically one fits

$$\chi^2 = (\mathbf{d}' - \widehat{\mathbf{W}}\mathbf{t} - a\,\mathbf{u}')^T \mathbf{C}'^{-1} (\mathbf{d}' - \widehat{\mathbf{W}}\mathbf{t} - a\,\mathbf{u}'), \tag{24}$$

where

$$\widehat{\mathbf{W}} = \mathbf{M}\left(\mathbf{W} + \mathbf{u}\mathbf{v}^T\right), \qquad \mathbf{u}' = \mathbf{M}\mathbf{u}. \tag{25}$$

The matrix $\mathbf{M}$ is optimized so that the transformed window is as compact as possible in theory k, while keeping the transformed covariance close to diagonal and preserving the information content of the likelihood [16]. In words, the method does not change the cosmological information; it repackages that information into a basis where the window is much better behaved.

In the DESI DR1 measurement paper, the official full-shape power-spectrum measurements used for cosmology are those labelled "θ-cut+rotated+RIC+AIC", where RIC and AIC denote radial and angular integral-constraint corrections estimated separately from mocks [14, 15].

1.5. **What students should remember.** There are three important conceptual lessons here. First, the survey window is part of the forward model, not an afterthought. Second, once the theory is discretized, the window operation is simply linear algebra. Third, when the estimator or the observing strategy produces a window with long tails, it is often better to change basis or redefine the estimator than to force the perturbation-theory model to predict arbitrarily small scales. The DESI BAO and full-shape pipelines are excellent modern examples of this philosophy in action.

2. The measurements of BAO

2.1. **BAO using power spectrum multipoles.** The template:

$$\alpha_\perp = \frac{D_A(z) r_d^{\rm fid}}{D_A^{\rm fid}(z) r_d}, \quad \alpha_\parallel = \frac{H^{\rm fid}(z) r_d^{\rm fid}}{H(z) r_d} \tag{26}$$

$$P_g(k,\mu) = P_{\rm nw}(k,\mu)\left\{1 + O(k) e^{-k^2\left[\mu^2\Sigma_\parallel^2 + (1-\mu^2)\Sigma_\perp^2\right]/2}\right\} \tag{27}$$

$$P_{\rm nw}(k,\mu) = B^2\left(1+\beta\mu^2\right)^2 P_{\rm nw,lin}(k) F(k,\mu) \tag{28}$$

$$F(k,\mu) = \frac{1}{(1 + k^2\mu^2\Sigma_s^2/2)} \tag{29}$$

$$P_\ell(k) = \left(\frac{r_s^{\rm fid}}{r_s}\right)^3 \frac{2\ell+1}{2\alpha_\perp^2\alpha_\parallel}\int_{-1}^{1} {\rm d}\mu P_g\left(k',\mu'\right)\mathcal{L}_\ell(\mu) + \frac{a_{\ell 1}}{k^3} + \frac{a_{\ell 2}}{k^2} + \frac{a_{\ell 3}}{k} + a_{\ell 4} + a_{\ell 5} k$$

$$\begin{aligned} k' &= \frac{k(1+\epsilon)}{\alpha}\left\{1 + \mu^2\left[(1+\epsilon)^{-6} - 1\right]\right\}^{1/2} \\ \mu' &= \frac{\mu}{(1+\epsilon)^3}\left\{1 + \mu^2\left[(1+\epsilon)^{-6} - 1\right]\right\}^{-1/2} \end{aligned} \tag{30}$$

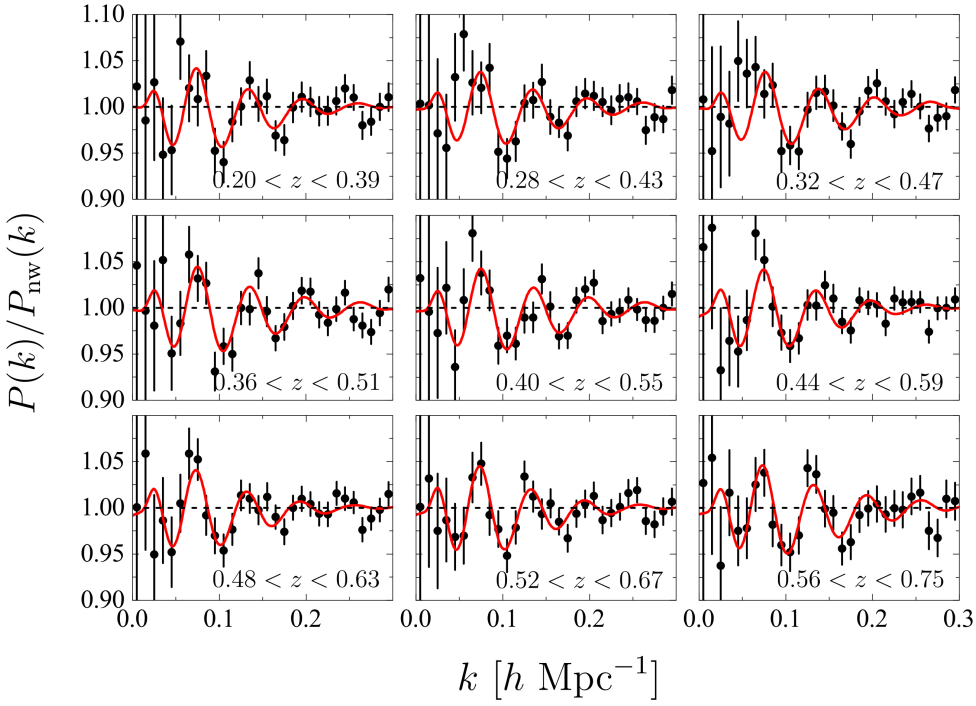

FIGURE 3. The BAO fit in k-space using BOSS DR12 data [6].

where

$$\alpha = \alpha_\perp^{2/3}\alpha_\parallel^{1/3}, \quad 1+\epsilon = \left(\frac{\alpha_\parallel}{\alpha_\perp}\right)^{1/3} \tag{31}$$

2.2. **BAO using correlation function multipoles.**

$$P_\ell(k) = \frac{2\ell+1}{2}\int_{-1}^{1} P(k,\mu)\mathcal{L}_\ell(\mu)d\mu \tag{32}$$

$$\xi_\ell(s) = \frac{i^\ell}{2\pi^2}\int k^2 P_\ell(k) j_\ell(ks)dk \tag{33}$$

$$\xi(s,\mu) = \sum_\ell \xi_\ell(s)\mathcal{L}_\ell(\mu) \tag{34}$$

$$\xi_\ell\left(s,\alpha_\perp,\alpha_\parallel\right) = \frac{2\ell+1}{2}\int_{-1}^{1}\xi\left(s',\mu'\right)\mathcal{L}_\ell(\mu)d\mu \tag{35}$$

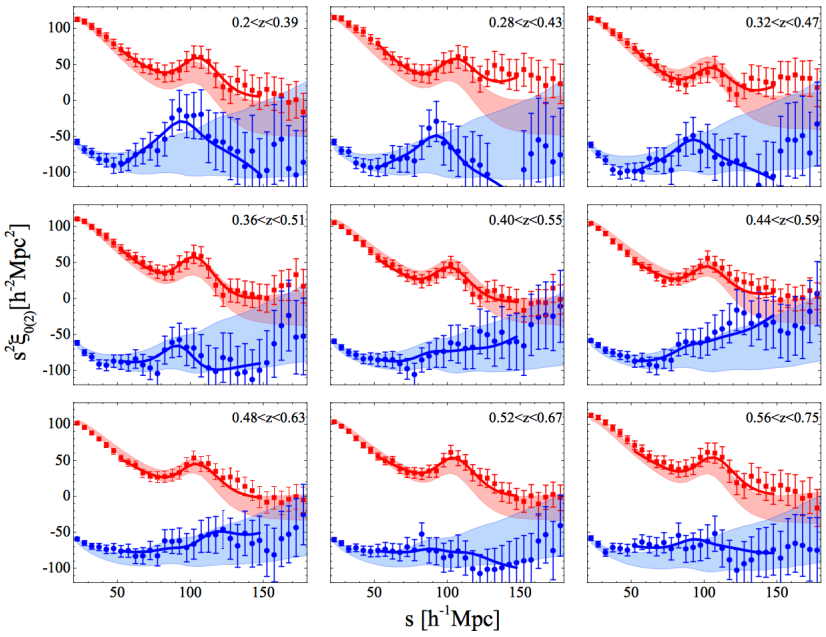

FIGURE 4. The BAO fit in s-space using BOSS DR12 data [7].

where

$$s' = s\sqrt{\mu^2\alpha_\parallel^2 + (1-\mu^2)\,\alpha_\perp^2};\ \mu' = \mu\alpha_\parallel/\sqrt{\mu^2\alpha_\parallel^2 + (1-\mu^2)\,\alpha_\perp^2} \tag{36}$$

$$A_\ell(s) = \frac{a_{\ell,1}}{s^2} + \frac{a_{\ell,2}}{s} + a_{\ell,3} \tag{37}$$

$$\begin{aligned} \xi_0^{\rm mod}(s) &= B_0\xi_0\left(s,\alpha_\perp,\alpha_\parallel\right) + A_0(s) \\ \xi_2^{\rm mod}(s) &= \xi_2\left(s,\alpha_\perp,\alpha_\parallel\right) + A_2(s) \end{aligned} \tag{38}$$

With this methodology, the BAO distance has been well measured from SDSS, 2dF [2, 3, 4, 5, 6, 7, 8] and DESI surveys [9, 10, 11], especially with the BAO-reconstruction technique [12, 13].

3. A compact DESI-style workflow for BAO fitting

A practical modern BAO analysis can be summarized as follows.

(1) Measure the clustering multipoles from data and random catalogs using the estimators introduced in Lecture 12.
(2) Build the survey window, either through the Hankel-transform route of Wilson et al. [1] or through a binned window matrix estimated from the random catalog and the chosen estimator [14, 9].
(3) Compute the unconvolved BAO model on a fine theory grid, keeping at least the multipoles that can leak into the observed data vector.
(4) Apply the survey window through a matrix multiplication, and only then compare to the measured band powers or correlation-function multipoles.
(5) If the estimator includes a small-angle cut or other operation that makes the window too extended in theory k, transform the data vector, covariance, and window matrix into a rotated basis before fitting [16, 14].
(6) Marginalize over broadband and observational nuisance terms and infer $(\alpha_\perp, \alpha_\parallel)$, or equivalently (α, ϵ), from the convolved model.

This completes the conceptual link between Lecture 12 and the present lecture. In Lecture 12 we learned how to measure two-point statistics from data and random catalogs. In the present lecture we learned how those measurements are compared to a theory model once the survey geometry and observational strategy have been folded in.

4. Summary

The original 2025 notes emphasized the elegant Hankel-transform treatment of the survey window and the standard BAO templates in Fourier and configuration space. The 2026 extension adds the complementary modern viewpoint used heavily in DESI: after discretization, the survey window is a matrix acting on a theory vector. This makes the convolution step transparent, fast, and easy to implement inside likelihood codes. It also makes clear why measured low-order multipoles receive leakage from higher-order theory multipoles.

The DESI DR1 analyses provide especially instructive examples. The galaxy BAO analysis uses direct window-matrix multiplication on a fine k grid [9]. The full-shape analysis goes one step further and rotates the power-spectrum data vector, covariance, and window matrix so that the effective window becomes more compact in theory k after the θ-cut used to control fiber-assignment incompleteness [16, 14, 15]. These ideas will remain central for Stage-IV survey analyses.

5. Suggested reading and exercises

For a first pass, students should read Wilson et al. [1] for the Hankel-transform formulation, DESI 2024 III [9] for the modern BAO implementation, and Pinon et al. [16] together with DESI 2024 II and V [14, 15] for the rotated-window method used in the DESI DR1 full-shape analysis.

Exercises.

- Starting from the continuous convolution, derive the binned matrix equation $P^{\rm obs}_{\ell,i} = \sum_{\ell',j} \mathcal{W}^{\ell\ell'}_{ij} P^{\rm th}_{\ell'}(k_j)$.
- Suppose your data vector contains only the monopole and quadrupole. Explain why it is still necessary to include $P_4(k)$ in the theory vector before the window multiplication.
- Show explicitly that for any invertible matrix $\mathbf{M}$, transforming $\mathbf{d}$, $\mathbf{C}$ and $\mathbf{W}$ as above leaves the Gaussian likelihood unchanged.
- In words, explain why a θ-cut can improve robustness against fiber assignment while simultaneously making the raw power-spectrum window matrix less diagonal.

Homework

This is a short homework set built around the main ideas of the lecture.

(1) **Alcock–Paczynski reparameterization.** Starting from

$$\alpha = \alpha_\perp^{2/3}\alpha_\parallel^{1/3}, \qquad 1+\epsilon = \left(\frac{\alpha_\parallel}{\alpha_\perp}\right)^{1/3},$$

derive the inverse relations

$$\alpha_\perp = \frac{\alpha}{1+\epsilon}, \qquad \alpha_\parallel = \alpha(1+\epsilon)^2.$$

Then evaluate $(\alpha_\perp, \alpha_\parallel)$ for $(\alpha, \epsilon) = (1.02, 0.01)$.

(2) **Block structure of the window matrix.** Suppose the measured data vector contains (P_0, P_2) in $N_d = 30$ k-bins, while the theory vector contains (P_0, P_2, P_4) on a fine grid with $N_t = 150$ points. Write the dimensions of $\mathbf{d}$, $\mathbf{t}$ and $\mathbf{W}$, and sketch the block form of $\mathbf{W}$. Which blocks encode leakage from higher multipoles into the observed monopole and quadrupole?

(3) **DESI-style forward model.** Write pseudocode for one likelihood evaluation in which you: (i) compute unconvolved theory multipoles on a fine k grid; (ii) stack them into a theory vector; (iii) apply the survey window by matrix multiplication; (iv) add broadband nuisance terms; and (v) evaluate χ^2 with the covariance matrix.

(4) **Why use a fine theory grid?** In a short paragraph, explain why DESI evaluates the unconvolved power spectrum on a k grid finer and broader than the fitted data vector before applying the window matrix. What can go wrong if the theory grid is too coarse or truncated too aggressively in k?

References

[1] M. J. Wilson, J. A. Peacock, A. N. Taylor and S. de la Torre, "Rapid modelling of the redshift-space power spectrum multipoles for a masked density field," Mon. Not. Roy. Astron. Soc. **464**, no. 3, 3121 (2017) doi:10.1093/mnras/stw2576 [arXiv:1511.07799 [astro-ph.CO]].

[2] D. J. Eisenstein *et al.* [SDSS], "Detection of the Baryon Acoustic Peak in the Large-Scale Correlation Function of SDSS Luminous Red Galaxies," Astrophys. J. **633**, 560-574 (2005) doi:10.1086/466512 [arXiv:astro-ph/0501171 [astro-ph]].

[3] S. Cole *et al.* [2dFGRS], "The 2dF Galaxy Redshift Survey: Power-spectrum analysis of the final dataset and cosmological implications," Mon. Not. Roy. Astron. Soc. **362**, 505-534 (2005) doi:10.1111/j.1365-2966.2005.09318.x [arXiv:astro-ph/0501174 [astro-ph]].

[4] W. J. Percival *et al.* [SDSS], "Baryon Acoustic Oscillations in the Sloan Digital Sky Survey Data Release 7 Galaxy Sample," Mon. Not. Roy. Astron. Soc. **401**, 2148-2168 (2010) doi:10.1111/j.1365-2966.2009.15812.x [arXiv:0907.1660 [astro-ph.CO]].

[5] S. Alam *et al.* [BOSS], "The clustering of galaxies in the completed SDSS-III Baryon Oscillation Spectroscopic Survey: cosmological analysis of the DR12 galaxy sample," Mon. Not. Roy. Astron. Soc. **470**, no.3, 2617-2652 (2017) doi:10.1093/mnras/stx721 [arXiv:1607.03155 [astro-ph.CO]].

[6] G. B. Zhao *et al.* [BOSS Collaboration], "The clustering of galaxies in the completed SDSS-III Baryon Oscillation Spectroscopic Survey: tomographic BAO analysis of DR12 combined sample in Fourier space," Mon. Not. Roy. Astron. Soc. **466**, no. 1, 762 (2017) doi:10.1093/mnras/stw3199 [arXiv:1607.03153 [astro-ph.CO]].

[7] Y. Wang *et al.* [BOSS Collaboration], "The clustering of galaxies in the completed SDSS-III Baryon Oscillation Spectroscopic Survey: tomographic BAO analysis of DR12 combined sample in configuration space," Mon. Not. Roy. Astron. Soc. **469**, no. 3, 3762 (2017) doi:10.1093/mnras/stx1090 [arXiv:1607.03154 [astro-ph.CO]].

[8] G. B. Zhao *et al.*, "The clustering of the SDSS-IV extended Baryon Oscillation Spectroscopic Survey DR14 quasar sample: a tomographic measurement of cosmic structure growth and expansion rate based on optimal redshift weights," Mon. Not. Roy. Astron. Soc. **482**, no. 3, 3497 (2019) doi:10.1093/mnras/sty2845 [arXiv:1801.03043 [astro-ph.CO]].

[9] A. G. Adame *et al.* [DESI], "DESI 2024 III: baryon acoustic oscillations from galaxies and quasars," JCAP **04**, 012 (2025) doi:10.1088/1475-7516/2025/04/012 [arXiv:2404.03000 [astro-ph.CO]].

[10] A. G. Adame *et al.* [DESI], "DESI 2024 IV: Baryon Acoustic Oscillations from the Lyman alpha forest," JCAP **01**, 124 (2025) doi:10.1088/1475-7516/2025/01/124 [arXiv:2404.03001 [astro-ph.CO]].

[11] M. Abdul Karim *et al.* [DESI], "DESI DR2 Results II: Measurements of Baryon Acoustic Oscillations and Cosmological Constraints," [arXiv:2503.14738 [astro-ph.CO]].

[12] D. J. Eisenstein, H. j. Seo, E. Sirko and D. Spergel, "Improving Cosmological Distance Measurements by Reconstruction of the Baryon Acoustic Peak," Astrophys. J. **664**, 675-679 (2007) doi:10.1086/518712 [arXiv:astro-ph/0604362 [astro-ph]].

[13] E. Paillas *et al.* [DESI], "Optimal reconstruction of baryon acoustic oscillations for DESI 2024," JCAP **01**, 142 (2025) doi:10.1088/1475-7516/2025/01/142 [arXiv:2404.03005 [astro-ph.CO]].

[14] A. G. Adame *et al.* [DESI], "DESI 2024 II: Sample Definitions, Characteristics, and Two-point Clustering Statistics," JCAP **07**, 017 (2025) doi:10.1088/1475-7516/2025/07/017 [arXiv:2411.12020 [astro-ph.CO]].

[15] A. G. Adame *et al.* [DESI], "DESI 2024 V: Full-Shape Galaxy Clustering from Galaxies and Quasars," JCAP **09**, 008 (2025) doi:10.1088/1475-7516/2025/09/008 [arXiv:2411.12021 [astro-ph.CO]].

[16] M. Pinon *et al.*, "Mitigation of DESI fiber assignment incompleteness effect on two-point clustering with small angular scale truncated estimators," JCAP **01**, 131 (2025) [arXiv:2406.04804 [astro-ph.CO]].